TOP1-DNA Trapping by Exatecan and Combination Therapy with ATR Inhibitor

Ukhyun Jo[1], Yasuhisa Murai[1,2], Keli K. Agama[1], Yilun Sun[1], Liton Kumar Saha[1], Xi Yang[1], Yasuhiro Arakawa[1], Sophia Gayle[3], Kelli Jones[3], Vishwas Paralkar[3], Ranjini K. Sundaram[4], Jinny Van Doorn[4], Juan C. Vasquez[5], Ranjit S. Bindra[4], Woo Suk Choi[6], and Yves Pommier[1]

ABSTRACT

Exatecan and deruxtecan are antineoplastic camptothecin derivatives in development as tumor-targeted-delivery warheads in various formulations including peptides, liposomes, polyethylene glycol nanoparticles, and antibody–drug conjugates. Here, we report the molecular pharmacology of exatecan compared with the clinically approved topoisomerase I (TOP1) inhibitors and preclinical models for validating biomarkers and the combination of exatecan with ataxia telangiectasia and Rad3-related kinase (ATR) inhibitors. Modeling exatecan binding at the interface of a TOP1 cleavage complex suggests two novel molecular interactions with the flanking DNA base and the TOP1 residue N352, in addition to the three known interactions of camptothecins with the TOP1 residues R364, D533, and N722. Accordingly, exatecan showed much stronger TOP1 trapping, higher DNA damage, and apoptotic cell death than the classical TOP1 inhibitors used clinically. We demonstrate the value of SLFN11 expression and homologous recombination (HR) deficiency (HRD) as predictive biomarkers of response to exatecan. We also show that exatecan kills cancer cells synergistically with the clinical ATR inhibitor ceralasertib (AZD6738). To establish the translational potential of this combination, we tested CBX-12, a clinically developed pH-sensitive peptide–exatecan conjugate that selectively targets cancer cells and is currently in clinical trials. The combination of CBX-12 with ceralasertib significantly suppressed tumor growth in mouse xenografts. Collectively, our results demonstrate the potency of exatecan as a TOP1 inhibitor and its clinical potential in combination with ATR inhibitors, using SLFN11 and HRD as predictive biomarkers.

Introduction

Camptothecin and its derivatives trap topoisomerase I (TOP1)-DNA cleavage complexes (TOP1ccs) by binding at the interface of the cleaved DNA and TOP1, resulting in TOP1ccs that cause DNA damage leading to cell death and inhibition of TOP1-mediated DNA relaxation (1). Clinical camptothecin derivatives such as topotecan and irinotecan are ubiquitously used to treat a broad range of cancers (2, 3). Exatecan (DX-8951f) was developed as a water-soluble camptothecin derivative with stronger inhibition of TOP1 activity and tumor suppression capability than the clinically approved camptothecin derivatives (4–6). However, its development as a single agent was ceased due to dose-limiting side effects, and the absence of therapeutic benefits in combination with gemcitabine compared with gemcitabine alone in clinical testing (7).

Exatecan is being reevaluated in the context of tumor-targeted drug delivery approaches as TOP1-based antibody–drug conjugates (ADCs) appear less toxic than pyrrolobenzodiazepine DNA cross-linking- and microtubule inhibitor derivative–based ADCs (8–14). Deruxtecan, a close derivative of exatecan is already successfully used as a cytotoxic payload (15) conjugated with a HER2 targeting antibody in Trastuzumab Deruxtecan (Enhertu, T-DXd/DS-8201a), which has recently been clinically approved for the treatment of HER2-expressing solid tumors (16). A second TOP1 ADC, sacituzumab govitecan (Trodelvy, IMMU-132) based on SN-38, the active metabolite of irinotecan (2) and targeting TROP2 (17) has also been recently approved for triple-negative breast cancers (18). Exatecan is being investigated as the cytotoxic payload on a novel HER2-targeting ADC (9). Mechanistically, targeting tumor antigens enables the release of the cytotoxic camptothecin derivative specifically to cancerous cells, stabilizing the drug in the bloodstream until its delivery to the tumor (8, 19). Because clinical applications of ADC delivery are limited by subsets of cancers expressing high levels of antigen and off-target toxicity, the exatecan-based drug conjugate CBX-12 is being developed to improve drug delivery to a broad range of tumors while minimizing toxicity to normal tissues (14). CBX-12 is a pH-sensitive peptide conjugate that releases exatecan into tumor cells due to the acidic pH of the tumor microenvironment (14).

Clinical camptothecin derivatives are modified in the A and B rings of the camptothecin structure to increase their potency as TOP1cc poisons and their water solubility (**Fig. 1A**; ref. 20). Exatecan bears an additional amino benzyl ring appended to the A and B rings over positions 7 and 9 and has additional substitutions with a methyl and a fluorine group at positions 10 and 11, respectively. However, the mechanistic and therapeutic benefits of these modifications have not been fully documented in comparison with SN-38, the active

[1]Developmental Therapeutics Branch and Laboratory of Molecular Pharmacology, Center for Cancer Research, National Cancer Institute, Bethesda, Maryland. [2]Department of Gastroenterology and Hematology, Hirosaki University Graduate School of Medicine, Hirosaki, Japan. [3]Cybrexa Therapeutics, New Haven, Connecticut. [4]Department of Therapeutic Radiology, Yale School of Medicine, New Haven, Connecticut. [5]Department of Pediatrics, Yale School of Medicine, New Haven, Connecticut. [6]Laboratory of Molecular Biology, National Institute of Diabetes and Digestive and Kidney Diseases, NIH, Bethesda, Maryland.

Note: Supplementary data for this article are available at Molecular Cancer Therapeutics Online (http://mct.aacrjournals.org/).

Corresponding Authors: Yves Pommier and Ukhyun Jo, Center for Cancer Research, Developmental Therapeutics Branch & Laboratory of Molecular Pharmacology, National Cancer Institute, Building 37, Room 5068, Bethesda, MD 20892-4255. Phone: 240-760-6142; Fax: 240-541-4475; E-mail: pommier@nih.gov and ukhyun.jo@nih.gov

Mol Cancer Ther 2022;21:1090–102

doi: 10.1158/1535-7163.MCT-21-1000

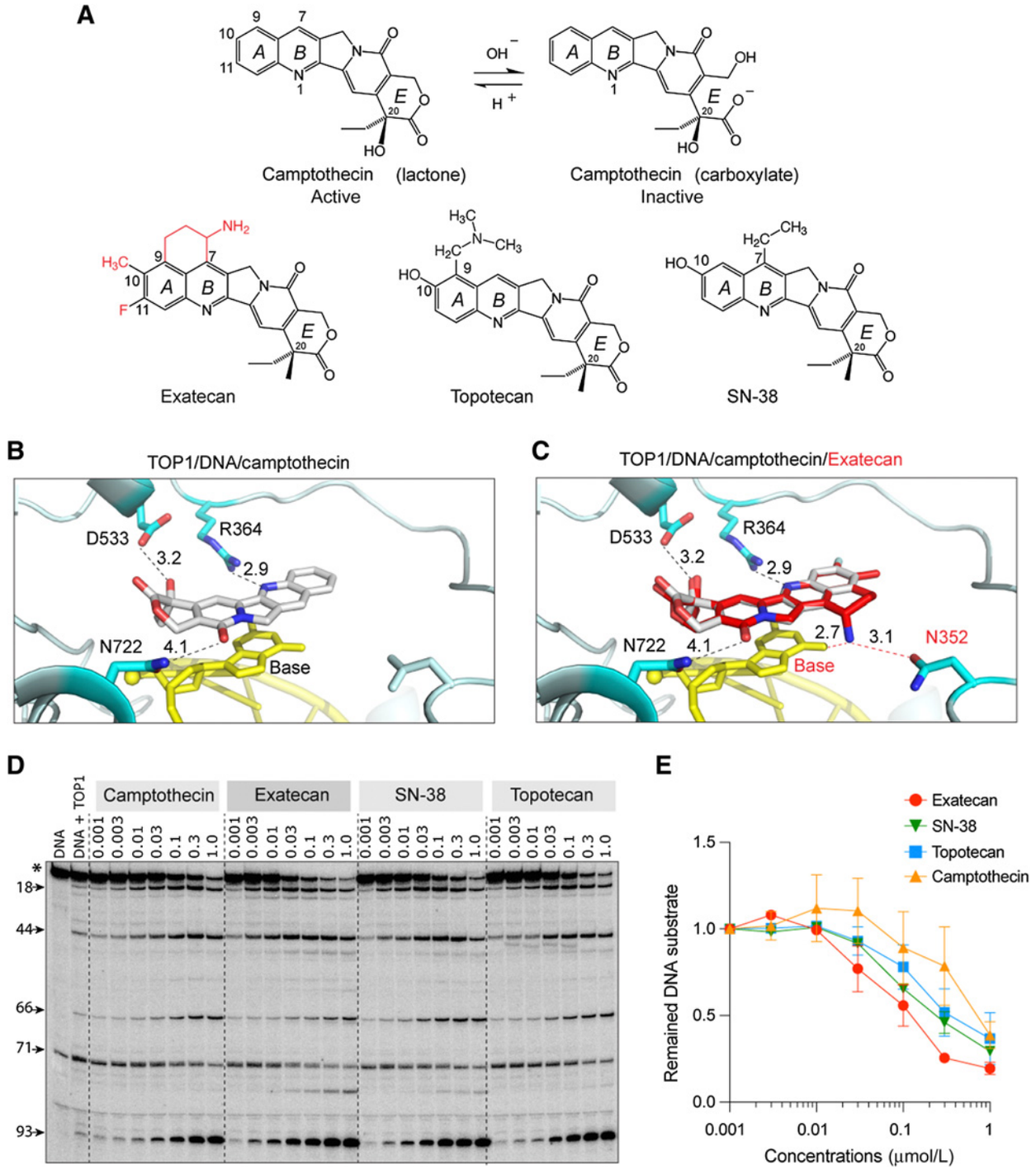

Figure 1.

Structural insights into the potent trapping of TOP1ccs by exatecan. **A,** Chemical structures of CPT and its clinical derivatives (exatecan, topotecan, and SN-38). **B,** Representative view of CPT (light grey) bound to human TOP1 (cyan) and DNA (yellow; PDB: 1T8I). In addition to base stacking, CPT makes three hydrogen bonds with TOP1 through D533, N722 and R364. The numbers indicate the distance of the bonds in Angstrom. **C,** Superposition of exatecan (red) and CPT (light grey) into the TOP1 (cyan)-DNA (yellow) structure. The two dotted lines (red) represent the potential additional hydrogen bonds of exatecan with the DNA base and N352 of TOP1. **D,** Comparative TOP1-mediated DNA cleavage (TOP1ccs) induced by exatecan and other TOP1 inhibitors. Recombinant TOP1 was incubated with 3′-end labeled 117 bp DNA oligo in the presence of the indicated drug concentrations. Fragmented DNA oligos were visualized on PAGE gel by using PhosphorImager (Molecular Dynamics). **E,** Quantitation of DNA substrates (*) as shown in panel **D** in duplicate experiments. Band intensity of the DNA substrate was determined by Image Quant software (Molecular Dynamics). CPT, camptothecin.

metabolite of irinotecan, which is the most active clinical derivative of camptothecin (20, 21).

Homologous recombination (HR) deficiency (HRD), as observed in *BRCA1* or *BRCA2* mutant settings, has recently been shown to serve as predictive biomarkers for TOP1 inhibitors (22, 23) in addition to their synthetic lethality with PARP inhibitors (24). Another emerging biomarker of response to both TOP1 inhibitors and PARP inhibitors is the putative DNA/RNA helicase/nuclease, Schlafen 11 (SLFN11; refs. 25, 26). Cancer cells expressing SLFN11 are selectively more vulnerable to treatment with clinical TOP1 inhibitors including camptothecin and noncamptothecin derivatives (22, 25). Yet, in the large proportion (approximately 50%) of cancer cells that do not express SLFN11, combination treatment with inhibitors of the replication checkpoint ataxia telangiectasia and Rad3-related kinase (ATR) has recently been shown to overcome resistance to TOP1 inhibitors (27, 28).

In the current study, we elucidate the molecular mechanisms underlying the anticancer potency of exatecan. We demonstrate the selective susceptibility in HRD and SLFN11 expressing cancer cells to exatecan, and validate the synergy of the exatecan conjugate CBX-12 with the ATR inhibitor ceralasertib (AZD6738) in cell culture and human xenografts (29).

Materials and Methods

Cell lines and reagents

DU145 (ATCC, HTB-81) and DU145-SLFN11 knockout (KO) cells were grown in DMEM medium with 10% FBS/1% penicillin-streptomycin. MOLT-4 (ATCC, CRL-1582), MOLT-4-SLFN11 KO, CCRF-CEM (ATCC, CCL-119), CCRF-CEM-SLFN11 KO, DMS114 (ATCC, CRL-2066), DMS114-SLFN11 KO, and HCT-116 (ATCC, CCL-247) cells were grown in RPMI1640 medium with 10% FBS/1% penicillin-streptomycin. DU145, MOLT-4, CCRF-CEM, DMS114, and HCT-116 were purchased from the ATCC. All SLFN11 KO cells were established in our laboratory (30). DT40, DT40-BRCA1 KO, and DT40-BRCA2 KO cells (gifts from Dr. S. Takeda, Kyoto University, Kyoto, Japan) were grown in RPMI1640 medium supplemented with 1% chicken serum, 10 nmol/L β-mercaptoethanol, 10% FBS, and 1% penicillin-streptomycin. UWB1.289 and UWB1.289+BRCA1 cells (gifts from Dr. J. Lee, NCI) were cultured in complete growth medium (50% RPMI1640 medium, 50% MEGM medium with 10% FBS/1% penicillin-streptomycin. camptothecin, exatecan, topotecan, SN-38, LMP400, talazoparib, and ceralasertib (AZD6738) were acquired from the Developmental Therapeutics Program (DCTD, NCI). CBX-12 was obtained from Cybrexa Therapeutics. All cell lines were passaged 15 times and examined by MycoAlert *Mycoplasma* Detection Kit (Lonza).

Modeling of exatecan in the TOP1cc

The structural coordinates of exatecan (PubChem: 151115), camptothecin (PubChem: 24360), SN-38 (PubChem: 443154), and topotecan (PubChem: 60700) were downloaded from the NCBI-PubChem Compound (http://www.ncbi.nlm.nih.gov/pccompound) database in three-dimensional SDF-file format and then were converted to PDB format using PyMOL (ver.2.3.5., www.pymol.org). The spatial localization of TOP1-DNA-inhibitor [camptothecin/PDB: 1T8I (31) and topotecan/PDB: 1K4T (32)] within the three-dimensional structures with the distances between molecules was graphically presented using PyMOL. Structural superposition modeling was carried out by overlapping exatecan to the bound camptothecin in the TOP1-DNA structure using CooT (33) and PyMOL. Docking simulations and estimated binding affinity of TOP1 inhibitors were performed using AutoDock Vina v.1.1.2.

TOP1-mediated DNA cleavage assay

A 3′-[^{32}P]-labeled 117-bp DNA substrate oligonucleotide (34) was incubated with recombinant human TOP1 (purified from insect cells using a baculovirus construct for the full-length human TOP cDNA; ref. 35) in 20-μL reaction buffer (10 mmol/L Tris-HCl, pH 7.5, 50 mmol/L KCl, 5 mmol/L MgCl2, 0.1 mmol/L EDTA, and 15 μg/mL BSA) at 30°C for 20 minutes in the presence of the indicated drug concentrations. Reactions were terminated by adding SDS (0.5% final concentration) followed by the addition of two volumes of loading dye (80% formamide, 10 mmol/L sodium hydroxide, 1 mmol/L sodium EDTA, 0.1% xylene cyanol, and 0.1% bromophenol blue). Aliquots of reaction mixtures were subjected to 16% denaturing PAGE. Gels were dried and visualized by using PhosphorImager and Image Quant software (Molecular Dynamics).

Detection of cellular TOP1ccs

DNA-trapped TOP1 was determined by a modified rapid approach to DNA adduct recovery (RADAR) assay (36). After treatment of TOP1 inhibitors, DU145 cells (1×10^6 cells/sample) were washed with 1x PBS and lysed with 600 μL of DNAzol (Invitrogen), followed by precipitation with 300 μL of 200-proof ethanol by centrifugation at 14,000 rpm. The nucleic acids were collected, washed with 75% ethanol, resuspended in 200 μL of TE buffer, and then heated at 65°C for 15 minutes, followed by shearing with sonication (40% output for 10-second pulse and 10-second rest repeated four times). The samples were centrifuged at 15,000 rpm for 5 minutes at 4°C, and the supernatant was collected. The sample (1 μL) was saved for spectrophotometric measurement of absorbance at 260 nm to quantitate DNA content (NanoDrop). Two μg of each sample was subjected to slot-blot for immunoblotting with anti-TOP1 antibody (No. 556597, BD Biosciences) or anti-dsDNA antibody (No. 3519, Abcam) as a loading control. The intensity of TOP1 and DNA was quantified by densitometric analysis using ImageJ.

Immunofluorescence microscopy

DU145 cells were plated in 6-well plates on sterilized coverslips and treated the next day with either DMSO as a vehicle or different concentrations (indicated in figure legends) of the TOP1 inhibitors exatecan and topotecan for 2 hours. After washing with 1xPBS, cells were fixed with 4% paraformaldehyde in 1xPBS for 15 minutes at room temperature. Subsequent permeabilization was performed in 2.5% Triton-X/1xPBS for 15 minutes before 1xPBS washing and 1-hour blocking in 5% BSA/1xPBS. Coverslips were then incubated for 1 hour with mouse anti–phospho-Histone H2AX (Ser139) antibody (No. 05-636, Millipore), diluted 1:500 in 5% BSA/1xPBS. After three washes with 1xPBS, samples were incubated with secondary antibody (Alexa Fluor 488, goat anti-mouse, diluted 1:2,000 in 5% BSA/1xPBS for 1 hour in the dark. Coverslips were washed (3 × 5 minutes in 1xPBS), stained with DAPI, and mounted using VECTASHIELD (Vector Laboratories). Images were captured with a Zeiss LSM 880 super-resolution microscope with a 63x objective lens. The signal intensity was quantified by Image J software.

Alkaline comet assay

DNA single- and double-stranded breaks were determined by the Alkaline CometAssay Kit (Trevigen) according to the manufacturer's protocol. Briefly, after treatment with the TOP1 inhibitors, cells were harvested, washed in 1xPBS, and combined at 3×10^5 cells/mL with

molten LMAagrose in a 1:10 (v/v) ratio. Fifty μL of the combined mixture was added onto the comet slide. After the gel was solidified at 4°C, slides were immersed in 4°C lysis solution for 30 minutes and subsequently incubated in alkaline unwinding solution for 20 minutes at room temperature in the dark. Alkaline electrophoresis was carried out at 1 V/cm and 300 mA for 40 minutes at 4°C. Slides were rinsed twice in deionized H2O for 5 minutes each, then in 70% ethanol for 5 minutes and air-dried overnight. DNA was stained with 100-μL SYBR Gold for 30 minutes, briefly rinsed in water, and allowed to air-dry. Fluorescent signals were visualized using fluorescence microscopy and quantified by using ImageJ plugin OpenComet (version 1.3).

Apoptotic cell death

Cells were seeded on 6-well plates (3×10^5 cells/well) and treated with drugs for 24 hours and 48 hours. After harvest, cells were examined with the ApoDETECT Annexin V-FITC kit according to the manufacturer's protocol (Invitrogen) and analyzed by flow cytometry using a FACS Canto (Becton Dickinson) and FlowJo software.

Western blotting

Cells were lysed with NETN300 buffer [1% NP40, 300 mmol/L NaCl, 0.1 mmol/L EDTA, and 50 mmol/L Tris (pH 7.5)] supplemented with protease inhibitor cocktail (Cell Signaling Technology). For TOP1 degradation, cells were incubated in alkaline lysis buffer (200 mmol/L NaOH, 2 mmol/L EDTA) and samples neutralized with neutralization buffer (1M HCl, 600 mmol/L Tris, pH 8.0). Subsequently, cell lysates were incubated in nuclease digestion buffer (5 mmol/L $CaCl_2$, 50 mmol/L Tris-HCl, pH 8.0). After adding SDS-PAGE sample buffer or 2X boiling lysis buffer (50 mmol/L Tris-HCl pH 6.8, 2% SDS, 850 mmol/L β-mercaptoethanol), samples were resolved by SDS-PAGE gels (Novex Tris-Glycine Mini Gels, Invitrogen) and transferred onto polyvinylidene difluoride membranes (Millipore). Membranes were immunoblotted with the following antibodies: TOP1 (No. 556597, BD Biosciences), GAPDH (GTX100118; GeneTex), PARP (9542; Cell signaling Technology), and cleaved caspase-3 (9661; Cell signaling Technology). After overnight incubation, membranes were incubated with the species-appropriate horseradish peroxidase–conjugated secondary antibodies for 1 hour. Protein signals were visualized by ChemiDoc MP Imaging System (Bio-Rad) with SuperSignal West Pico PLUS Chemiluminescent Substrate (Thermo Scientific). Signal intensity was quantified with the Image J software.

Cell viability

Cells were plated in 96-well white plates at a density of 2,000 cells/well in 100-μL complete growth medium. Cells were incubated with TOP1 inhibitors for 72 hours. Cell viability was determined by CellTiter-Glo Luminescent Cell Viability Assay (Promega) according to the manufacturer's protocol. Briefly, the reaction solution was added at 50 μL/well and the plates were kept in the dark for 10 minutes with mild shaking, and then luminescence was measured by Envision 2104 Multi-label Microplate Reader (Perkin Elmer).

Xenograft studies

For MDA-MB-231 xenografts, 3- to 4-week-old female athymic nude Foxn^{nu} mice (HSD: Athymic nude-Foxn1^{nu}, Envigo Labs) were inoculated subcutaneously with MDA-MB-231 tumor cells (1×10^6) combined 1:1 with Matrigel (Corning, 47743-716) in a total volume of 0.1 mL. Once the tumors reached a mean volume of 50 to 100 mm^3, mice were randomized into treatment groups ($n = \pm 10$ mice/arm) and treated as indicated. CBX-12 (Cybrexa Therapeutics) doses were prepared by diluting DMSO stocks in 5% (w/v) mannitol in citrate vehicle, as described (14). CBX-12 doses were administered intraperitoneally at 10 mg/kg once daily for 4 days, repeated weekly for 3 weeks. Ceralasertib (AZD6738) doses were prepared by diluting DMSO stocks in 10% (w/v) 2-hydroxy-propyl-b-cyclodextrin (Sigma No. H107) vehicle. Ceralasertib doses were then administered via oral gavage at 25 mg/kg once daily for 5 days, repeated weekly for 3 weeks. For HCT-116 xenografts, 6-week-old female athymic nude Foxn^{nu} mice were obtained from Taconic Labs (Catalog No. NCRNU-F). Each mouse was inoculated subcutaneously with HCT-116 tumor cells (2.5×10^6) with Matrigel (1:1). After tumors had grown to a mean size of approximately 100 to 200 mm^3, the mice were then split into groups ($n = \pm 10$ mice/arm) and treated as indicated. CBX-12 doses were administered intraperitoneally at 5 mg/kg once daily for 4 days, repeated weekly for 3 weeks. Ceralasertib doses were administered via oral gavage at 25 mg/kg once daily for 21 days. Mice were followed for the 3 weeks of treatment and throughout the subsequent 3-week washout period. Tumor volumes were measured twice weekly with calipers and calculated according to the formula for ellipsoid volume: $\pi/6 \times (\text{tumor length}) \times (\text{tumor width})^2$. Mice with tumors exceeding 2 cm^3 in volume or exhibiting significant weight loss or tumor ulceration were euthanized, in accordance with institutional protocols. All animal studies were approved by the Institutional Animal Use and Care Committee and performed by the Guide for the Care and Use of Laboratory Animals.

Statistical analyses

Statistical analysis was calculated using two-tailed unpaired Student *t* test, one-way ANOVA with using the GraphPad Prism 8 software (GraphPad Software, La Jolla, CA, USA).

Data availability

The data generated in this study are available within the article and its Supplementary Data files.

Results

TOP1cc trapping by exatecan

As interfacial inhibitors (1), camptothecin and its derivatives trap TOP1ccs by π−π stacking with the base pairs flanking the DNA cleavage site and by three hydrogen bonds with TOP1 residues (R364, D533 and N722; **Fig. 1B**; Supplementary Fig. S1A; ref. 37). Because exatecan possesses an amino benzyl ring between the A and B rings (**Fig. 1A**), we hypothesized that these modifications may form additional interactions with the TOP1 and DNA complex. To test this hypothesis, we modeled and superimposed exatecan onto the structure of the TOP1-DNA-camptothecin complex (PDB: 1T8I; **Fig. 1C**). We found that the amino group of the benzyl ring was positioned to make two additional hydrogen bonds with the +1 DNA base oxygen and the N352 residue of TOP1, implying enhanced binding affinity of exatecan compared with camptothecin (Supplementary Fig. S1B). These results show that exatecan can be readily modeled in the TOP1cc, and that it may form additional interaction that would stabilize its binding at the interface of TOP1-DNA complex to a greater extent than camptothecin, topotecan, and SN-38.

To test this possibility further, we measured the trapping of TOP1ccs by exatecan by performing DNA cleavage assays with recombinant TOP1 and ^{32}P-labeled DNA oligonucleotides. As shown in **Fig. 1D** and **E**, and Supplementary S1C, exatecan induced DNA cleavage more effectively than the other clinical TOP1 inhibitors tested: camptothecin, SN-38, and topotecan. Together, these results

establish that exatecan is a potent TOP1 poison, acting at low nanomolar concentrations.

We also confirmed that CBX-12, which is a pH-sensitive peptide–exatecan conjugate (14), acts as a prodrug. As shown in Supplementary Fig. S1D, CBX-12 was at least 100 times less active than exatecan in the induction of DNA cleavage by recombinant human TOP1.

Exatecan induces cellular TOP1ccs and induces TOP1 degradation at nanomolar concentrations

To confirm the potency of exatecan as a TOP1 poison, we examined the level of DNA-trapped TOP1 in comparison with clinical TOP1 inhibitors topotecan, SN-38, and camptothecin using a modified RADAR assay. Exatecan was the most potent drug and induced TOP1ccs at a lower concentration (0.03 μmol/L) than the other TOP1 inhibitors (**Fig. 2A** and **B**; Supplementary S2A and S2B).

Given that DNA-trapped TOP1 is rapidly removed from DNA and degraded by the ubiquitin-proteasome pathway (38), we hypothesized that exatecan may produce faster cellular TOP1 degradation than the other TOP1 inhibitors. To demonstrate this, we first treated cells with the TOP1 inhibitors for 2 hours and then allowed the cells to grow without drugs for 30 minutes to allow the reversal of TOP1ccs and TOP1 degradation. As expected, exatecan induced TOP1 degradation in a dose-dependent manner and appeared markedly more effective than the other clinical TOP1 inhibitors, SN-38 and topotecan (**Fig. 2C** and **D**).

Collectively, these results show that exatecan is a potent TOP1 inhibitor, inducing cytotoxic TOP1ccs leading to the degradation of TOP1 at nanomolar concentrations.

Exatecan causes cellular DNA breakage and apoptotic cell death

Given that TOP1 inhibitor-mediated TOP1ccs lead to DNA damage (20), we determined the induction of phosphorylated H2AX (γH2AX), a sensitive biomarker for DNA double-strand breaks, in cells treated with exatecan in comparison with topotecan. As shown in **Fig. 3A** and **B**; Supplementary Fig. S3A, γH2AX was induced by exatecan at 10 nmol/L drug concentration and increased in a dose-dependent manner. The induction of γH2AX by topotecan was significantly less than that of exatecan.

Next, DNA break induction by exatecan was examined using the comet assay. Exatecan produced DNA breaks in a dose-dependent manner and was significantly more effective than topotecan (Supplementary Fig. S3C and S3D).

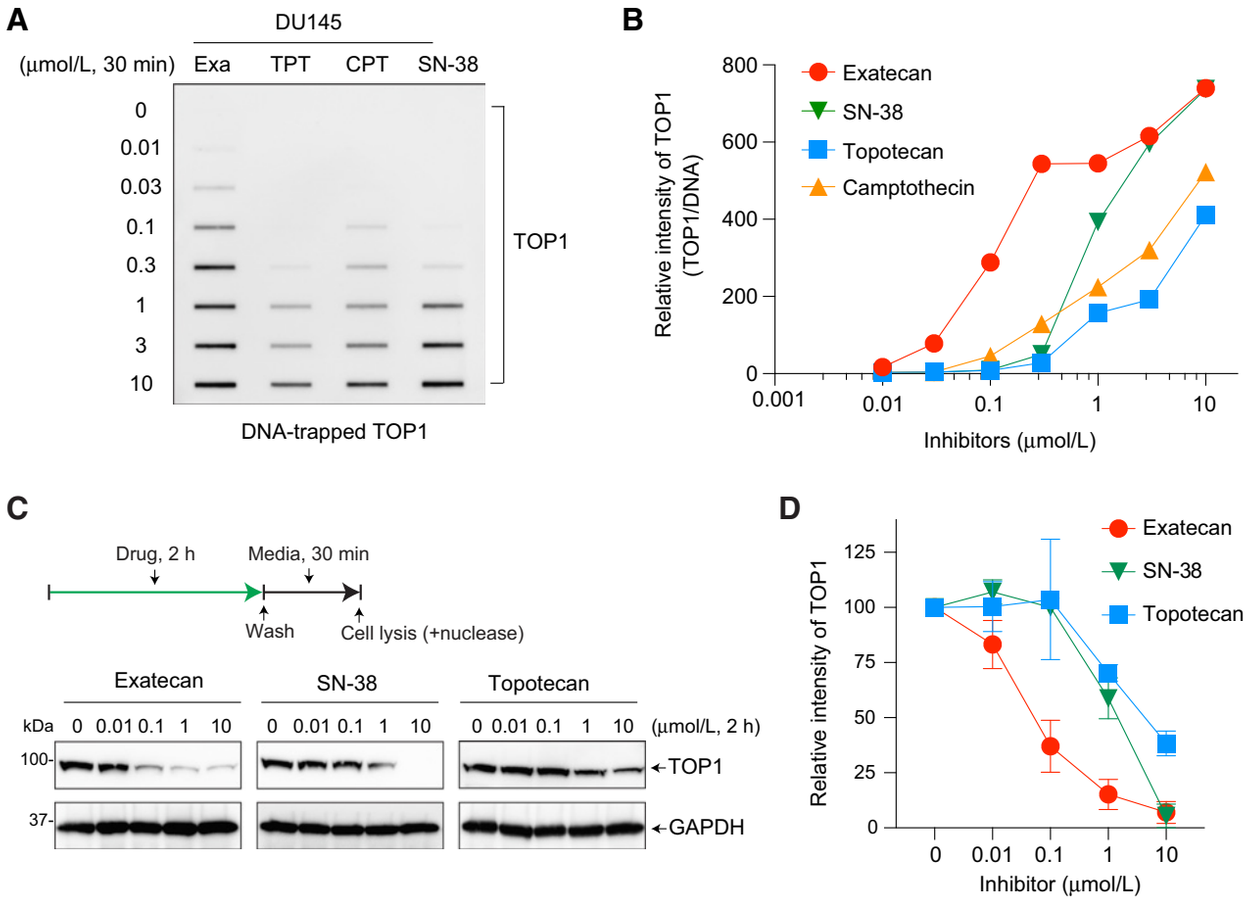

Figure 2.

Exatecan leads to greater TOP1-DNA trapping than topotecan, SN-38 and CPT. **A,** Detection of DNA-trapped TOP1 by exatecan and other TOP1 inhibitors. DU145 cells were treated with the indicated drug concentrations for 30 minutes. TOP1ccs were isolated by RADAR assay. **B,** Quantitation of TOP1ccs from panel **A** in a single experiment. The intensity of TOP1 was analyzed by ImageJ software and normalized to DNA loading. Data were plotted with GraphPad Prism 8. **C,** TOP1 degradation induced by exatecan. DU145 cells were incubated with the indicated TOP1 inhibitors for 2 hours. Following TOP1 reversal for 30 minutes without inhibitors, TOP1 levels were determined by Western blotting. **D,** Quantification of total cellular TOP1 bands in duplicate experiments. Band intensity was analyzed using the ImageJ software and normalized to GAPDH used as a loading control. CPT, camptothecin.

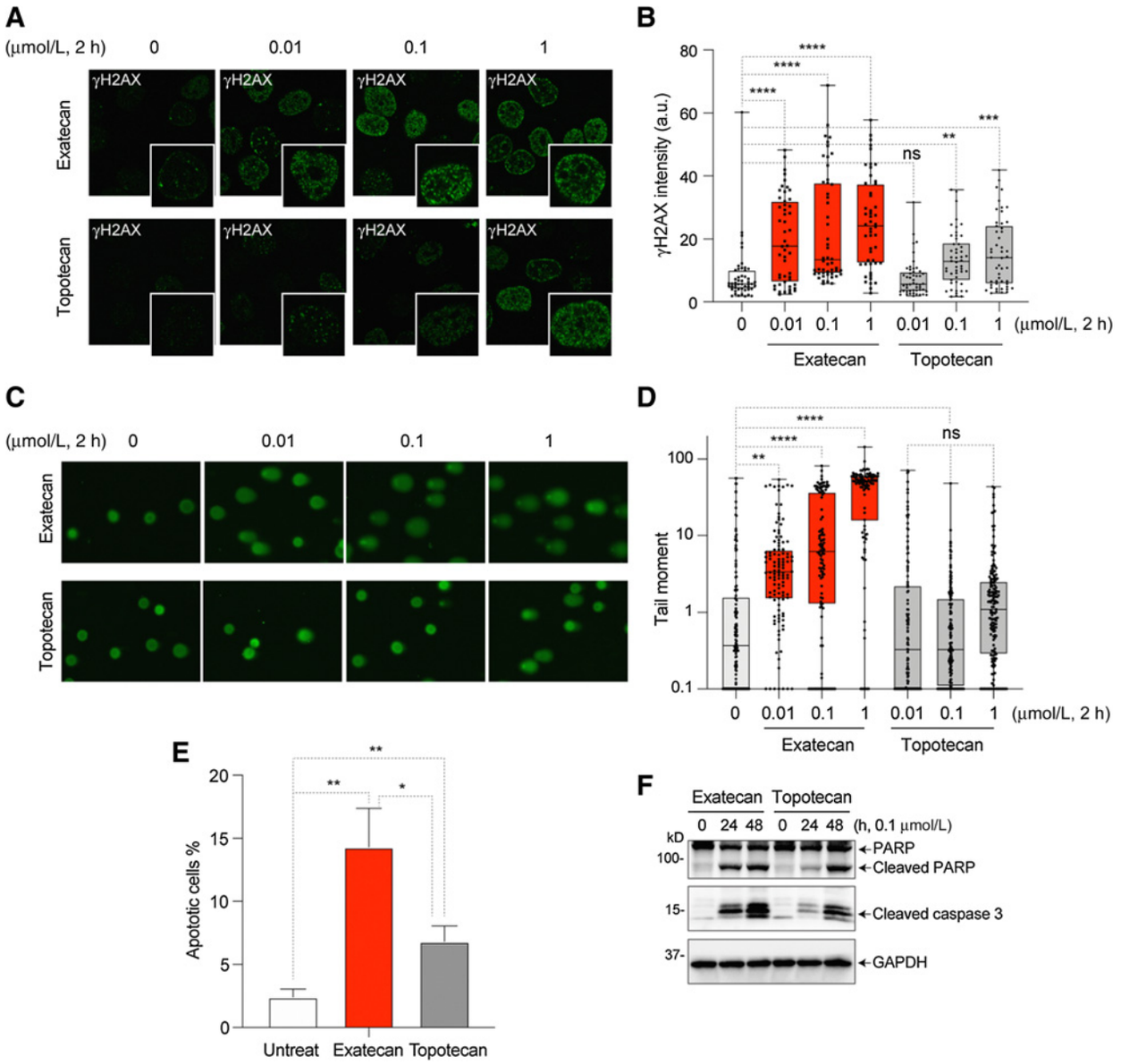

Figure 3.

DNA damage and cell death induced by exatecan. **A,** Representative immunofluorescence images of γH2AX (green) in exatecan- or topotecan-treated DU145 cells. **B,** Intensity of γH2AX fluorescence (average per cell) for the experiment depicted in panel A (mean ± SEM, $N = 50$/each) **, P value < 0.002; ***, P value < 0.0004; ****, P value < 0.0001; a.u., arbitrary units. **C,** Representative images of comet analysis in DU145 cells treated with exatecan and topotecan. **D,** Quantitation of tail moments of experiments depicted in panel **B** (mean ± SEM, $N = 100$/each) quantified with the Open Comet/ImageJ program. **, P value < 0.006, ****, P value < 0.0001. **E,** Apoptotic cell death induced by exatecan and topotecan and measured by Annexin V/PI staining. *, P value < 0.01; **, P value < 0.005. **F,** Cleavage of PARP1 and caspase-3 in exatecan and topotecan treated cells measured by Western blotting.

To determine whether the TOP1-induced DNA breaks generated by exatecan result in cell death, we measured apoptosis using Annexin V-FITC staining. As shown in **Fig. 3E** and Supplementary Fig. S3B, exatecan-treated cells exhibited higher apoptotic responses than the topotecan-treated cells. These findings were confirmed by detecting cleaved PARP and caspase 3 (**Fig. 3F**).

Exatecan is the most potent cytotoxic inhibitor among clinical TOP1 inhibitors

Because of the higher levels of DNA damage and apoptosis induced by exatecan compared with topotecan, we tested the cytotoxicity of exatecan in comparison with the other clinical TOP1 inhibitors, topotecan, SN-38, and LMP400 (indotecan) in four different human

cancer cell lines: acute leukemia MOLT-4 and CCRF-CEM, prostate cancer DU145, and small cell lung cancer DMS114. As shown in **Fig. 4**, exatecan stood out as being significantly more active than the three other TOP1 inhibitors. IC_{50} values of exatecan were in the picomolar range against the four tested cancer cell lines and showed over 10 to 50 times higher potency of exatecan compared with the next best TOP1 inhibitor, SN-38 (**Fig. 4E**).

Susceptibility to exatecan is selectively increased in cancer cells expressing SLFN11 and with defective HR

Given that SLFN11 expression is a dominant biomarker of response to TOP1cc-targeting chemotherapeutic agents, which kill cancer cells under replicative stress (26), we compared the activity of exatecan in four pairs of *SLFN11*-KO isogenic cancer cell lines: prostate DU145, acute leukemia CCRF-CEM, acute leukemia MOLT-4, and small cell

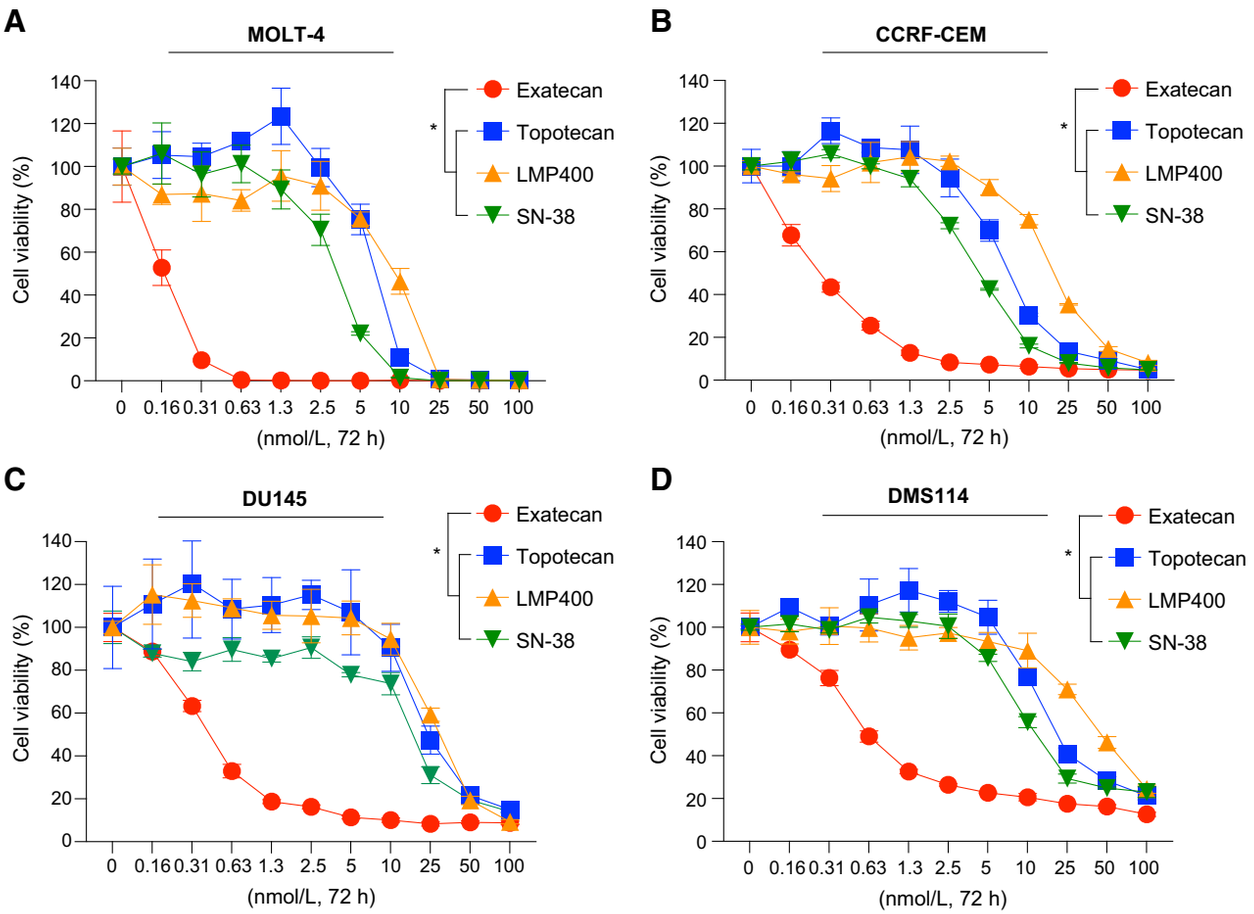

E

Cell line	Exatecan IC_{50} (95% CI)	SN-38 IC_{50} (95% CI)	Topotecan IC_{50} (95% CI)	LMP400 IC_{50} (95% CI)	Relative ratio of IC_{50} (Inhibitor/exatecan)		
					SN-38	Topotecan	LMP400
MOLT-4	0.16 (0.16–0.16)	2.96 (2.70–3.24)	5.33 (4.53–6.19)	8.62 (7.37–10.04)	18.50	33.31	53.88
CCRF-CEM	0.25 (0.23–0.26)	3.63 (3.44–3.84)	5.32 (4.46–6.34)	14.04 (12.13–16.25)	14.52	21.28	56.16
DU145	0.49 (0.46–0.52)	13.90 (10.87–17.31)	17.57 (13.82–22.09)	22.47 (19.39–25.86)	28.55	35.86	45.86
DMS114	0.58 (0.52–0.65)	8.19 (7.54–8.90)	12.10 (10.14–14.51)	26.06 (21.42–31.32)	14.12	20.86	44.93

Figure 4.

Exatecan is the most potent TOP1 inhibitor. **A–D,** Cytotoxicity of clinical TOP1 inhibitors (exatecan, SN-38, topotecan, and LMP400) in MOLT-4, CCRF-CEM, DU145, and DMS114 cells. Cells were treated as indicated for 72 hours and cell viability was measured by CellTiter-Glo assay. Error bars represent standard deviations in the triplicate. Statistical values were calculated using one-way ANOVA with Dunnett multiple comparisons test. *, *P* value < 0.03. **E,** IC_{50} values of the TOP1 inhibitors calculated by GraphPad Prism 8. The IC_{50} values represent the mean (nM) obtained from triplicate experiments in MOLT-4, CCRF-CEM, DMS114, and DU145 cells. CI, confidence interval. Ratios indicate comparative IC_{50} values between exatecan and the other TOP1 inhibitors.

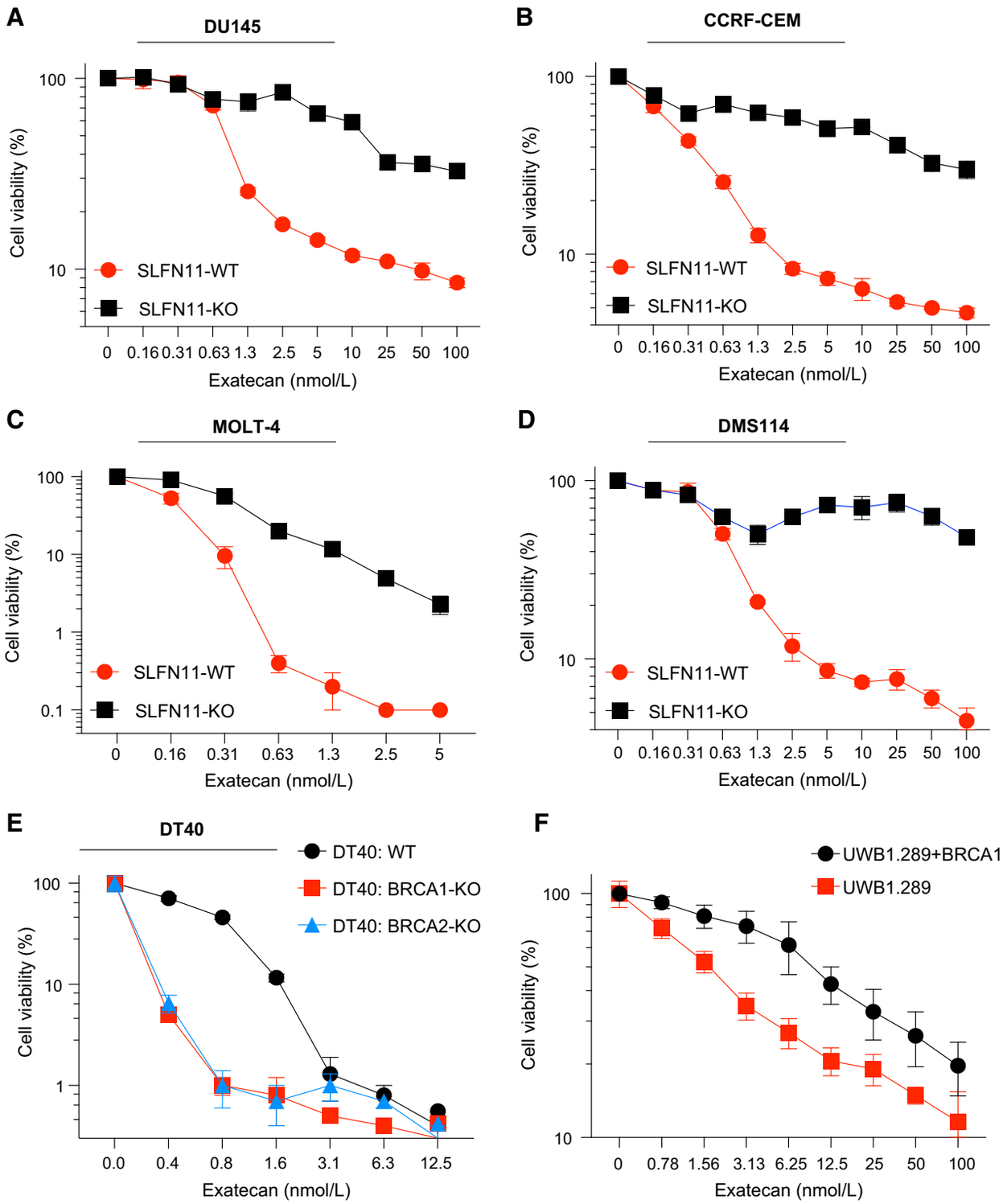

Figure 5.

SLFN11-proficient and HR-deficient cells are preferentially vulnerable to exatecan. **A–D,** Cytotoxicity of exatecan in the isogenic DU145, CCRF-CEM, MOLT-4, DMS114, and paired SLFN11 KO cells. Cells were treated as indicated for 72 hours and cell viability was measured by CellTiter-Glo assay. **E,** Cytotoxicity of exatecan in the isogenic DT40 chicken B cells and paired BRCA1/2 KO cells. Cells were treated as indicated for 72 hours and cell viability was measured by CellTiter-Glo assay. **F,** Cytotoxicity of exatecan in UWB1.289 (carrying a BRCA1 mutation, BRCA1-null) and UWB1.289+BRCA1 cells. Cells were treated as indicated for 72 hours, and cell viability was measured by e CellTiter-Glo assay. Error bars represent standard deviations in the triplicate.

lung cancer DMS114. As expected, SLFN11-positive cancer cells were consistently more sensitive to exatecan than their isogenic SLFN11-negative cells counterpart (**Fig. 5A–D**), which confirms the potential value of SLFN11 expression as a predictive biomarker for exatecan-based therapies.

In addition to SLFN11, HRD increases susceptibility to TOP1 inhibitors because of defective DNA repair (22, 23). To determine whether HRD enhances chemosensitivity to exatecan, we tested cell viability in BRCA1-KO and BRCA2-KO genetically altered DT40 cell lines, which are derived from chicken B-cell lymphoma. As expected, exatecan was more potent than topotecan and SN-38 in DT40 cells (Supplementary Fig. S4A–S4C), as observed in the human cancer cells (**Fig. 4**). We also confirmed that cell killing in BRCA1-KO and BRCA2-KO DT40 cells by exatecan was significantly higher than in DT40 parental wild-type (WT) cells (**Fig. 5E**). These results were further validated in the BRCA1-null human ovarian cancer cell line UWB1.289, in which complementation with WT BRCA1 partially reversed chemosensitivity to exatecan (**Fig. 5F**), indicating that HR status is a potential predictive biomarker for the clinical use of exatecan.

Exatecan synergizes with ATR inhibitor

To our knowledge, no studies of exatecan with other clinical chemotherapeutic drugs have been reported since the unsuccessful combination clinical trial with gemcitabine (7). Given that topotecan and camptothecin show consistent synergy with ATR inhibitors (27, 28, 39), we studied the cytotoxicity of combination treatments of exatecan with the ATR inhibitor ceralasertib (AZD6738), which is being developed in various clinical trials (40, 41). To do so, we tested exatecan with minimally toxic doses of ceralasertib (0.5 and 1 μmol/L) as a single treatment. As shown in **Fig. 6A** and **B**, low doses of combination with ceralasertib enhanced the cytotoxicity of exatecan in human MDA-MB-231 breast cancer and HCT-116 colon cancer cells, which are both *SLFN11*-negative (http://discover.nci.nih.gov/cellminercdb). Combination index computation showed strong synergistic effects of ceralasertib for a range of concentrations of exatecan, implying that combination with low doses of ATR inhibitors could be used for cancer treatment in the clinic (**Fig. 6C** and **D**).

Antitumor activity of CBX-12, a pH-sensitive peptide–exatecan conjugate, as a single agent and with the ATR inhibitor ceralasertib in mouse xenograft models

CBX-12 is a pH-sensitive alphalex-exatecan conjugate currently being tested in early-phase clinical trials (14). Alphalex is a tumor-targeting technology consisting of a unique variant of a family of pH-Low Insertion Peptides that enables the targeting of acidic cell surfaces (42). In CBX-12, it makes exatecan specifically target the surface of cancer cells while avoiding exposure to the active payload in the vascular system and reducing cytotoxicity to normal

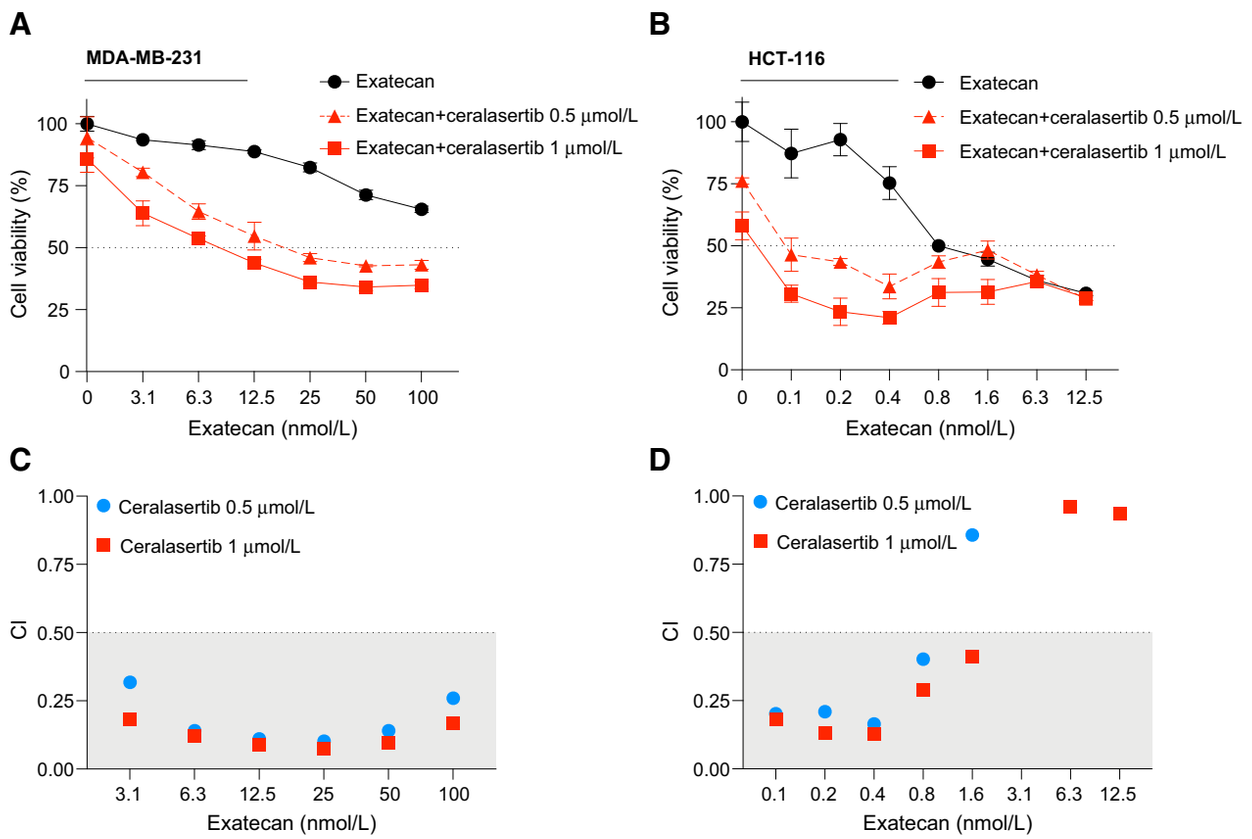

Figure 6.

Exatecan synergizes with the ATR inhibitor ceralasertib. **A** and **B,** Cytotoxicity of combination treatments of exatecan with ATR inhibitor. Human breast cancer MDA-MB-231 and colon adenocarcinoma HCT116 cells were treated with the indicated concentrations of exatecan without or with ceralasertib (0.5 and 1 μmol/L) for 72 hours, and cell viability was measured by CellTiter-Glo assays. Error bars represent standard deviations in the triplicate. **C** and **D,** Combination index (CI) plots for the combinations exatecan and ceralasertib from data obtained from panels **A** and **B**. The CI values were calculated by using CompuSyn. Additive combination: 0.5 < CI < 1, and synergistic combinations: 0 < CI < 0.5.

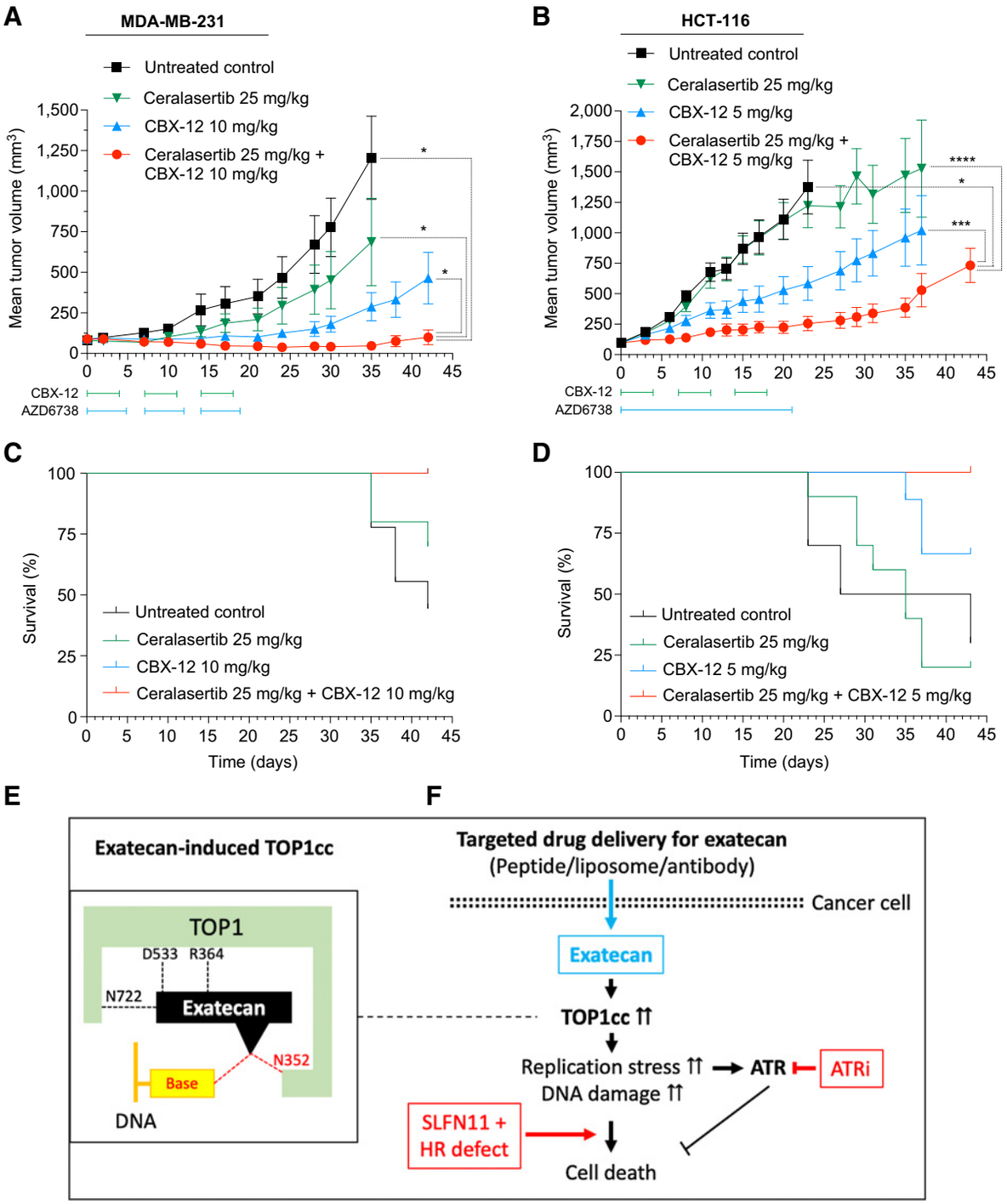

Figure 7.

Antitumor activity of CBX-12 in human breast cancer and colon cancer xenografts and synergy with the ATR inhibitor ceralasertib. **A** and **B,** Tumor suppression by CBX-12 without and with ceralasertib (AZD6738) in MDA-MB-231 and HCT-116 xenografts. MDA-MB-231 xenografts (**A**) were treated with CBX-12 intraperitoneally at 10 mg/kg once daily for 4 days, repeated weekly for 3 weeks. Ceralasertib was administered via oral gavage at 25 mg/kg once daily for 5 days, repeated weekly for 3 weeks. HCT-116 xenografts (**B**) were treated with CBX-12 intraperitoneally at 5 mg/kg once daily for 4 days, repeated weekly for 3 weeks. Ceralasertib doses were then administered via oral gavage at 25 mg/kg once daily for 21 days. Tumor volumes are shown as mean ± SEM ($N = 10$ mice for each group). Statistical values were calculated using one-way ANOVA with Dunnett multiple comparisons test. *, P value < 0.05; ***, P value < 0.001; ****, P value < 0.0001. **C** and **D,** Cell survival after drug treatments for the MDA-MB-231 (**C**) and HCT-116 (**D**) xenografts. **E,** Proposed model for potent TOP1cc trapping by exatecan. **F,** Therapeutic strategy and predictive biomarkers for targeted exatecan delivery. ATRi, ATR inhibitor; HR, homologous recombination including BRCA1/2; SLFN11, Schlafen 11 expression.

cells. To validate our previous results with CBX-12 in preclinical settings, we tested the antitumor activity of CBX-12 alone and in combination with ceralasertib in MDA-MB-231 and HCT116 xenograft (**Fig. 7A–D**). Combination treatment significantly inhibited tumor growth without significant toxicity in both mouse xenografts compared with CBX-12 and ceralasertib monotherapy without significant toxicity (**Fig. 7A** and **B**). Overall survival of mice treated with the combination was also better than that of CBX-12 alone and ceralasertib single treatment (**Fig. 7C** and **D**). No significant body weight loss was noted in the single-agent or combination groups, highlighting a lack of combination toxicity due to tumor-selective delivery of exatecan by CBX-12 (Supplementary Fig. S5A and S5B). The dose of ceralasertib chosen is in the range of that used frequently in the preclinical settings. Preclinical efficacy of ceralasertib in combination with chemotherapy appears to translate in the clinical setting, as recent early phase I data show preliminary signs of efficacy (NCT02630199). Thus, these results suggest that combining CBX-12 and ceralasertib may be a potentially new treatment approach that warrants further investigation.

Discussion

In this study, we report the molecular pharmacology and outstanding potency of exatecan in comparison with the classical TOP1 inhibitors, camptothecin, topotecan, and SN-38 (the active metabolite of irinotecan) and provide proof-of-concept pharmacodynamic (γH2AX) and clinical biomarkers (SLFN11 and HRD) to support the ongoing clinical investigations of exatecan as payload for targeted drug delivery systems (2, 14, 19, 43). Consistent with our data, exatecan initially showed much stronger antitumor activity in multiple preclinical studies, promising better therapeutic benefits than the other clinical TOP1-targeted drugs (44–46). However, the high potency of exatecan as a free drug led to dose-limiting cytotoxicity and hindered its development as a new clinically applicable TOP1 poison (14). Here, we studied the underlying molecular pharmacology of exatecan. We also provide preclinical evidence of combination strategies with CBX-12, a peptide–exatecan conjugate, and ATR inhibitors as a strategy to overcome the limitations of free exatecan.

We demonstrate that exatecan leads to stronger TOP1 trapping than SN-38, topotecan or camptothecin in biochemical and cellular assays and that CBX-12 acts as a prodrug for exatecan. We propose that this enhanced trapping may result from additional molecular interactions with DNA and TOP1 (**Fig. 7E**). By docking simulation, we find that the amino group on the 6th amino benzyl ring of exatecan can form two additional molecular interactions with the oxygen of the +1 DNA base and the TOP1 residue (N352) in addition to three known interactions of camptothecin derivatives with the three TOP1 residues R364, D533, and N722 at the interface of the TOP1-DNA complex (31). Consistently, cells with a TOP1 mutation N352A have been reported to be resistant to a camptothecin derivative with a 10-OH substitution on the camptothecin A-ring. In addition, by analyzing The Cancer Genome Atlas with cBioPortal, we found that a patient with lung adenocarcinoma harbored a mutation at this same E352 residue (E352K; ref. Supplementary Fig. S5C), implying its potential clinical relevance for drug resistance. Furthermore, a mutant (E418K) of TOP1 at the TOP1cc interface and near the N352 residue has been detected in a patient with triple-negative breast cancer resistant to sacituzumab govitecan (47). These observations suggest the potential value of sequencing the *TOP1* gene in patients treated with exatecan to analyze potential drug resistance.

Although TOP1 inhibitors are widely used in the clinic as first-line chemotherapy, predictive biomarkers are not a current focus of attention. Although TOP1 overexpression and TDP1 deficiency have been proposed as potential predictive biomarkers (48), they are not systematically analyzed. Alternatively, SLFN11 has emerged as a dominant prediction biomarker for TOP1 inhibitors (25, 26). The results presented here are consistent with this possibility, as we show in four different isogenic cancer cell line models with *SLFN11*-WT and -KO, that SLFN11-expressing cancer cells are selectively sensitive to exatecan, as observed with other clinical TOP1 inhibitors (25, 49). Thus, evaluation of SLFN11 expression should be considered as a correlative factor for patient response to exatecan-based treatment, such as CBX-12. Ultimately, SLFN11 expression could be considered to select patients who may derive therapeutic benefits from exatecan-based cancer therapy. Here we also provide evidence that the relative resistance of SLFN11-negative cancer cells such as the breast cancer cell line MDA-MB-231 and the colon cancer cell line HCT-116 (ref. 50; http://discover.nci.nih.gov/cellminercdb; see **Figs. 6** and **7**), can be overcome by combination with the ATR inhibitor ceralasertib (**Fig. 7F**). In addition to SLFN11 expression, we confirmed that cancer cells with HRD are also selectively vulnerable to the exatecan (23). Thus, therapeutic strategies taking into account SLFN11 expression and HRD should enable the use of exatecan to aim accurately precision medicine (**Fig. 7F**; ref. 2).

Recent attempts to combine a carrier and the cytotoxic warhead exatecan have provided new opportunities to overcome the therapeutic limitations of exatecan in the clinic, which are due to exatecan's very high potency as a TOP1 poison (19, 43). Cancer cell–specific targeting with the exatecan derivative Deruxtecan has shown remarkable results in multiple clinical trials, which led to the FDA approval of trastuzumab deruxtecan (Enhertu; ref. 16). These results illustrate the possibility that exatecan can be re-formulated to harness its antineoplastic properties while limiting the toxicity (9, 44). In particular, the newly developed pH-sensitive peptide–exatecan conjugate, CBX-12, showed that it can target most cancer cells regardless of limited oncogenic antigen expression observed in the antibody conjugation (14). CBX-12 selectively delivers exatecan to cancer cells in their low pH environment while sparing normal tissues and thereby shows better antitumor activity compared with nonconjugated exatecan itself in preclinical models. In two different mouse xenograft models, we show that CBX-12 significantly suppresses tumor growth as monotherapy and even more efficiently in combination with the ATR inhibitor ceralasertib, in line with previous data showing a synergistic effect with CBX12 and the PARP inhibitor talazoparib (14).

In conclusion, our data uncover mechanistic insight into the nature of exatecan-induced TOP1cc as the most potent TOP1 poison and a therapeutic rationale for exatecan-based therapy via a drug-targeted system in combination with clinical ATR inhibitors. We also provide evidence for predictive clinical (SLFN11 and HRD) and pharmacodynamic (γH2AX) biomarkers that may improve the efficacy of exatecan.

Authors' Disclosures

R.S. Bindra is a co-founder and consultant for Cybrexa Therapeutics during the conduct of the study. No disclosures were reported by the other authors.

Authors' Contributions

U. Jo: Conceptualization, investigation, writing–original draft. **Y. Murai:** Investigation. **K.K. Agama:** Investigation. **Y. Sun:** Investigation. **L.K. Saha:** Investigation. **X. Yang:** Investigation. **Y. Arakawa:** Investigation. **S. Gayle:**

Investigation, writing–original draft. **K. Jones:** Investigation. **V. Paralkar:** Investigation, writing–original draft. **R.K. Sundaram:** Investigation. **J. Van Doorn:** Investigation, writing–original draft. **J.C. Vasquez:** Investigation, writing–original draft. **R.S. Bindra:** Investigation, writing–original draft. **W.S. Choi:** Investigation. **Y. Pommier:** Conceptualization, supervision, funding acquisition, writing–original draft, writing–review and editing.

Acknowledgments

Our studies are funded by the Center for Cancer Research, the intramural program of the NCI (Z01-BCC006150). J.C. Vasquez is funded in part by the Robert Wood Johnson Harold Amos Medical Faculty Development Program and the Fund to Retain Clinical Scientists at Yale, sponsored by the Doris Duke Charitable Foundation award No. 2015216, and the Yale Center for Clinical Investigation. Y Murai is supported by the Sakurai Memorial Fund for Medical Research at Hirosaki University and JSPS KAKENHI Grant (JP21K20887).

The costs of publication of this article were defrayed in part by the payment of page charges. This article must therefore be hereby marked *advertisement* in accordance with 18 U.S.C. Section 1734 solely to indicate this fact.

Received December 10, 2021; revised February 18, 2022; accepted April 12, 2022; published first April 19, 2022.

References

1. Pommier Y, Marchand C. Interfacial inhibitors: targeting macromolecular complexes. Nat Rev Drug Discov 2011;11:25–36.
2. Thomas A, Pommier Y. Targeting topoisomerase I in the era of precision medicine. Clin Cancer Res 2019;25:6581–9.
3. Kopetz S, Guthrie KA, Morris VK, Lenz HJ, Magliocco AM, Maru D, et al. Randomized trial of irinotecan and cetuximab with or without vemurafenib in BRAF-mutant metastatic colorectal cancer (SWOG S1406). J Clin Oncol 2021; 39:285–94.
4. Mitsui I, Kumazawa E, Hirota Y, Aonuma M, Sugimori M, Ohsuki S, et al. A new water-soluble camptothecin derivative, DX-8951f, exhibits potent antitumor activity against human tumors *in vitro* and *in vivo*. Jpn J Cancer Res 1995;86:776–82.
5. Joto N, Ishii M, Minami M, Kuga H, Mitsui I, Tohgo A. DX-8951f, a water-soluble camptothecin analog, exhibits potent antitumor activity against a human lung cancer cell line and its SN-38–resistant variant. Int J Cancer 1997;72:680–6.
6. Vey N, Giles FJ, Kantarjian H, Smith TL, Beran M, Jeha S. The topoisomerase I inhibitor DX-8951f is active in a severe combined immunodeficient mouse model of human acute myelogenous leukemia. Clin Cancer Res 2000; 6:731–6.
7. Abou-Alfa GK, Letourneau R, Harker G, Modiano M, Hurwitz H, Tchekmedyian NS, et al. Randomized phase III study of exatecan and gemcitabine compared with gemcitabine alone in untreated advanced pancreatic cancer. J Clin Oncol 2006;24:4441–7.
8. Beck A, Goetsch L, Dumontet C, Corvaia N. Strategies and challenges for the next generation of antibody–drug conjugates. Nat Rev Drug Discov 2017;16: 315–37.
9. Conilh L, Fournet G, Fourmaux E, Murcia A, Matera EL, Joseph B, et al. Exatecan antibody–drug conjugates based on a hydrophilic polysarcosine drug-linker platform. Pharmaceuticals 2021;14:247.
10. Takegawa N, Nonagase Y, Yonesaka K, Sakai K, Maenishi O, Ogitani Y, et al. DS-8201a, a new HER2-targeting antibody–drug conjugate incorporating a novel DNA topoisomerase I inhibitor, overcomes HER2-positive gastric cancer T-DM1 resistance. Int J Cancer 2017;141:1682–9.
11. Iwata TN, Ishii C, Ishida S, Ogitani Y, Wada T, Agatsuma T. A HER2-targeting antibody–drug conjugate, trastuzumab deruxtecan (DS-8201a), enhances antitumor immunity in a mouse model. Mol Cancer Ther 2018; 17:1494–503.
12. Haratani K, Yonesaka K, Takamura S, Maenishi O, Kato R, Takegawa N, et al. U3-1402 sensitizes HER3-expressing tumors to PD-1 blockade by immune activation. J Clin Invest 2020;130:374–88.
13. Kotani D, Shitara K. Trastuzumab deruxtecan for the treatment of patients with HER2-positive gastric cancer. Ther Adv Med Oncol 2021;13: 1758835920986518.
14. Gayle S, Aiello R, Leelatian N, Beckta JM, Bechtold J, Bourassa P, et al. Tumor-selective, antigen-independent delivery of a pH sensitive peptide-topoisomerase inhibitor conjugate suppresses tumor growth without systemic toxicity. NAR Cancer 2021;3:zcab021.
15. Li W, Veale KH, Qiu Q, Sinkevicius KW, Maloney EK, Costoplus JA, et al. Synthesis and evaluation of camptothecin antibody–drug conjugates. ACS Med Chem Lett 2019;10:1386–92.
16. Keam SJ. Trastuzumab deruxtecan: first approval. Drugs 2020;80:501–8.
17. Goldenberg DM, Stein R, Sharkey RM. The emergence of trophoblast cell-surface antigen 2 (TROP-2) as a novel cancer target. Oncotarget 2018;9: 28989–9006.
18. Wahby S, Fashoyin-Aje L, Osgood CL, Cheng J, Fiero MH, Zhang L, et al. FDA approval summary: accelerated approval of sacituzumab govitecan-hziy for third-line treatment of metastatic triple-negative breast cancer. Clin Cancer Res 2021;27:1850–4.
19. Hafeez U, Parakh S, Gan HK, Scott AM. Antibody–drug conjugates for cancer therapy. Molecules 2020;25:4764.
20. Pommier Y. DNA topoisomerase I inhibitors: chemistry, biology, and interfacial inhibition. Chem Rev 2009;109:2894–902.
21. Tanizawa A, Fujimori A, Fujimori Y, Pommier Y. Comparison of topoisomerase I inhibition, DNA damage, and cytotoxicity of camptothecin derivatives presently in clinical trials. J Natl Cancer Inst 1994;86:836–42.
22. Marzi L, Szabova L, Gordon M, Weaver Ohler Z, Sharan SK, Beshiri ML, et al. The indenoisoquinoline TOP1 inhibitors selectively target homologous recombination–deficient and Schlafen 11–positive cancer cells and synergize with olaparib. Clin Cancer Res 2019;25:6206–16.
23. Coussy F, El-Botty R, Chateau-Joubert S, Dahmani A, Montaudon E, Leboucher S, et al. BRCAness, SLFN11, and RB1 loss predict response to topoisomerase I inhibitors in triple-negative breast cancers. Sci Transl Med 2020;12:eaax2625.
24. Lord CJ, Ashworth A. PARP inhibitors: Synthetic lethality in the clinic. Science 2017;355:1152–8.
25. Murai J, Thomas A, Miettinen M, Pommier Y. Schlafen 11 (SLFN11), a restriction factor for replicative stress induced by DNA-targeting anticancer therapies. Pharmacol Ther 2019;201:94–102.
26. Jo U, Murai Y, Takebe N, Thomas A, Pommier Y. Precision oncology with drugs targeting the replication stress, ATR, and Schlafen 11. Cancers 2021;13: 4601.
27. Jo U, Senatorov IS, Zimmermann A, Saha LK, Murai Y, Kim SH, et al. Novel and highly potent ATR Inhibitor M4344 kills cancer cells with replication stress, and enhances the chemotherapeutic activity of widely used DNA-damaging agents. Mol Cancer Ther 2021;20:1431–41.
28. Thomas A, Takahashi N, Rajapakse VN, Zhang X, Sun Y, Ceribelli M, et al. Therapeutic targeting of ATR yields durable regressions in small cell lung cancers with high replication stress. Cancer Cell 2021;39:566–79.
29. Yap TA, Krebs MG, Postel-Vinay S, El-Khouiery A, Soria JC, Lopez J, et al. Ceralasertib (AZD6738), an Oral ATR kinase inhibitor, in combination with carboplatin in patients with advanced solid tumors: a phase I study. Clin Cancer Res 2021;27:5213–24.
30. Murai J, Feng Y, Yu GK, Ru Y, Tang SW, Shen Y, et al. Resistance to PARP inhibitors by SLFN11 inactivation can be overcome by ATR inhibition. Oncotarget 2016;7:76534–50.
31. Staker BL, Feese MD, Cushman M, Pommier Y, Zembower D, Stewart L, et al. Structures of three classes of anticancer agents bound to the human topoisomerase I-DNA covalent complex. J Med Chem 2005;48:2336–45.
32. Staker BL, Hjerrild K, Feese MD, Behnke CA, Burgin AB Jr, Stewart L. The mechanism of topoisomerase I poisoning by a camptothecin analog. Proc Natl Acad Sci U S A 2002;99:15387–92.
33. Emsley P, Lohkamp B, Scott WG, Cowtan K. Features and development of Coot. Acta Crystallogr D Biol Crystallogr 2010;66:486–501.
34. Dexheimer TS, Pommier Y. DNA cleavage assay for the identification of topoisomerase I inhibitors. Nat Protoc 2008;3:1736–50.
35. Laco GS, Du W, Kohlhagen G, Sayer JM, Jerina DM, Burke TG, et al. Analysis of human topoisomerase I inhibition and interaction with the cleavage site +1 deoxyguanosine, via *in vitro* experiments and molecular modeling studies. Bioorg Med Chem 2004;12:5225–35.

36. Kiianitsa K, Maizels N. A rapid and sensitive assay for DNA-protein covalent complexes in living cells. Nucleic Acids Res 2013;41:e104.
37. Pommier Y, Cushman M. The indenoisoquinoline noncamptothecin topoisomerase I inhibitors: update and perspectives. Mol Cancer Ther 2009;8: 1008–14.
38. Sun Y, Saha LK, Saha S, Jo U, Pommier Y. Debulking of topoisomerase DNA-protein crosslinks (TOP-DPC) by the proteasome, non-proteasomal, and non-proteolytic pathways. DNA Repair 2020;94:102926.
39. Bradbury A, Hall S, Curtin N, Drew Y. Targeting ATR as cancer therapy: a new era for synthetic lethality and synergistic combinations? Pharmacol Ther 2020; 207:107450.
40. Yap TA, Krebs MG, Postel-Vinay S, El-Khouiery A, Soria JC, Lopez J, et al. Ceralasertib (AZD6738), an oral ATR kinase inhibitor, in combination with carboplatin in patients with advanced solid tumors: a phase I study. Clin Cancer Res 2021;27:5213–24.
41. Kim ST, Smith SA, Mortimer P, Loembe AB, Cho H, Kim KM, et al. Phase I study of ceralasertib (AZD6738), a novel DNA damage repair agent, in combination with weekly paclitaxel in refractory cancer. Clin Cancer Res 2021;27:4700–9.
42. Wyatt LC, Lewis JS, Andreev OA, Reshetnyak YK, Engelman DM. Applications of pHLIP technology for cancer imaging and therapy. Trends Biotechnol 2017; 35:653–64.
43. Khongorzul P, Ling CJ, Khan FU, Ihsan AU, Zhang J. Antibody--drug conjugates: a comprehensive review. Mol Cancer Res 2020;18:3–19.
44. Royce ME, Hoff PM, Dumas P, Lassere Y, Lee JJ, Coyle J, et al. Phase I and pharmacokinetic study of exatecan mesylate (DX-8951f): a novel camptothecin analog. J Clin Oncol 2001;19:1493–500.
45. Esteva FJ, Rivera E, Cristofanilli M, Valero V, Royce M, Duggal A, et al. A phase II study of intravenous exatecan mesylate (DX-8951f) administered daily for 5 days every 3 weeks to patients with metastatic breast carcinoma. Cancer 2003;98:900–7.
46. Sun FX, Tohgo A, Bouvet M, Yagi S, Nassirpour R, Moossa AR, et al. Efficacy of camptothecin analog DX-8951f (Exatecan Mesylate) on human pancreatic cancer in an orthotopic metastatic model. Cancer Res 2003;63:80–5.
47. Coates JT, Sun S, Leshchiner I, Thimmiah N, Martin EE, McLoughlin D, et al. Parallel genomic alterations of antigen and payload targets mediate polyclonal acquired clinical resistance to sacituzumab govitecan in triple-negative breast cancer. Cancer Discov 2021;11:2436–45.
48. Gilbert DC, Chalmers AJ, El-Khamisy SF. Topoisomerase I inhibition in colorectal cancer: biomarkers and therapeutic targets. Br J Cancer 2012;106: 18–24.
49. Zhang B, Ramkumar K, Cardnell RJ, Gay CM, Stewart CA, Wang WL, et al. A wake-up call for cancer DNA damage: the role of Schlafen 11 (SLFN11) across multiple cancers. Br J Cancer 2021;125:1333–40.
50. Zoppoli G, Regairaz M, Leo E, Reinhold WC, Varma S, Ballestrero A, et al. Putative DNA/RNA helicase Schlafen-11 (SLFN11) sensitizes cancer cells to DNA-damaging agents. Proc Natl Acad Sci U S A 2012;109: 15030–5.